

# **Structural behaviour of CFRP strengthened beam-column connections under monotonic and cyclic loading**

T. Tafsirojjaman <sup>a,b\*</sup>, Sabrina Fawzia <sup>a</sup>, David P Thambiratnam <sup>a</sup>

<sup>a</sup> School of Civil and Environmental Engineering, Faculty of Science and Engineering,  
Queensland University of Technology, 2 George Street, Brisbane, QLD 4000, Australia.

<sup>b</sup> Centre for Future Materials (CFM), School of Civil Engineering and Surveying, University  
of Southern Queensland, Toowoomba, QLD, 4350, Australia.

(\*Corresponding author: tafsirojjaman@hdr.qut.edu.au, Tel: 61746315553)

Email addresses: tafsirojjaman@hdr.qut.edu.au (T. Tafsirojjaman),

sabrina.fawzia@qut.edu.au (Sabrina Fawzia), d.thambiratnam@qut.edu.au (DP

Thambiratnam)

## **ABSTRACT**

Welded beam-column connections may be vulnerable to failure under cyclic loading conditions. These connections might require strengthening to resist static and cyclic loads as they may exhibit inadequate capacity due to the design errors or material properties degradation because of severe environmental effects or an increase in service loads. With this in mind, a series of full-scale experiments have been conducted to investigate the behaviour of the bare and strengthened welded beam-column connections under both monotonic and large-displacement cyclic loading. Carbon fibre reinforced polymer (CFRP) is used as the strengthening material in the present study along with epoxy adhesive as the bonding material. The experimental study conclusively showed the benefits of CFRP composites to improve the performance of welded connections under both monotonic and cyclic loadings. Under monotonic loading, the ultimate moment capacity, stiffness, dissipation of energy and ductility

of the welded connections improved by strengthening with CFRP. Additionally, under cyclic loading, the CFRP strengthened welded connections showed improvement in moment hysteresis behaviour, higher stiffness and energy dissipation capacity compared to their bare counterparts. Moreover, the experimentally obtained moment capacities match reasonably well with the theoretically predicted moment capacities.

**Keywords:** Welded beam-column connections; Strengthening; Carbon fibre reinforced polymer (CFRP); Monotonic loading; Cyclic loading.

## **1. Introduction**

Over the past two decades, Earthquakes have attributed to catastrophic losses in human lives and property and have adversely affected the economies of countries. This has led to the introduction of more stringent seismic building regulations and codes. However, existing structures may not meet certain requirements for seismic resistance, as observed during recent surveys following the 2010 Christchurch New Zealand earthquake [1]. In September 2010, an earthquake of 7.1 magnitude occurred in Christchurch, New Zealand. Five months later, a 6.3 magnitude aftershock occurred; this sequence resulted in approximately 185 deaths and 15 billion dollars of structural damage [1]. Old and new steel structures, including both low-rise and high-rise buildings, were damaged during the Northridge earthquake in 1994. Severe damage was found in many steel structures including the hospitals and other healthcare facilities. Damage in the welded beam-column connections was the most common scenario and only 25% of connections remained undamaged. There were instances where all the connections on certain floors suffered damage. Within the surveyed structures, approximately 70% of floors had a minimum of one severely damaged welded connection [2]. Local buckling and yielding of the girder's flanges and column buckling of the frames were noticed in several steel structures [3]. Welded connections possess good load carrying capacity hysteretic behaviour and prevent cumulative damage under seismic and cyclic loading but their fracture tendency

index is very low under seismic and cyclic loading [4]. It is therefore imperative to strengthen existing steel structures to enhance their performance during an earthquake. Under earthquake loads, which can be simulated through cyclic loading, inadequately designed structural steel members can suffer fatigue and cause cracks [5,6]. Failure of critical members in a steel building due to fracture can result in extensive damage to the buildings and this is a major concern for designers [5]. In addition to the seismic deficiency of existing structures and their fatigue damage, structural members in a steel building might require strengthening due to deterioration of material properties under adverse environmental conditions, an increase in the service loads or inadequate design of the steel members. To address these issues, extensive research has been required to conduct on the strengthening and rehabilitation of beam-column connections of steel structures.

Strengthening of metal members traditionally involves the welding of additional metal plates. Although beam-column connections reinforced with additional welded steel plates showed higher moment capacities and improvement in elastic stiffness values compared to the bare beam-column connections [7], this method is a time-consuming process, which also increases the dead weight of the existing structure. It also introduces the risk of steel deterioration because of corrosion under severe environmental conditions, since the protectants must be removed from the metal as a part of the welding process. The welding process also affects the stress distribution in the steel from the heat loading during the welding [5]. These issues have opened the field to alternative strengthening processes that avoid the aforementioned difficulties while improving the structural integrity of the steel member during earthquake events.

The engineering community has accepted research into adhesively bonded fibre reinforced polymer (FRP) as a strengthening method, due to its ability to overcome many of the drawbacks seen in traditional metal reinforcing methods. FRP's main benefits include high resistance to

corrosion [8], high tensile strength [9], high strength-weight ratio [10,11] and time-efficient installation [12]. When the FRP material has adhered to the metal plate surface, a composite action is created in the structure, as they deform together as one. Seismic strengthening of RC structures using FRP composites has received extensive attention and research in this area has confirmed that FRP strengthening is a very effective technique for seismic upgrading of RC frames [13–15]. FRP composites are very effective for upgrading RC structures subjected to seismic action as displacements can be reduced and strength capacity enhanced, both by up to 100% as a result of which sway column plastic-collapse mechanism can be prevented [14]. FRP strengthening techniques can also enhance the energy dissipation capacity and ductility and improve the global behaviour of under-designed RC structures by preventing brittle behaviour through the confinement of the column ends [15]. In recent times, researchers have also paid extensive attention to improve the seismic performances of steel frames [16–20]. CFRP strengthening technique was shown to improve the stiffness of the steel frame and reduced the tip deflection [16]. In addition, CFRP retrofitted steel frames showed higher energy dissipation capacity under seismic action compared to the bare steel frames [17] along with reductions in the inter-story drifts [18,19]. Overstrength and ductility also improved significantly in the FRP strengthened frames compared to their bare counterparts [20]. Recently there has been researched into retrofitting existing steel members with FRP to overcome strength deficiencies [21–26] and results have confirmed the benefits of FRP to repair or strengthen steel members. CFRP strengthened the circular hollow section (CHS) showed a higher load capacity compared to the bare section under pure bending [21] and four-point loading [22]. The moment capacity of cantilever circular hollow members under monotonic loading was also enhanced by CFRP strengthening [23]. Kabir et al. studied the durability of CHS members wrapped with CFRP under cold weather [24] and seawater [27] and confirmed the efficiency of CFRP wrapping. The local buckling behaviour of steel members was

effectively delayed by retrofitting with FRP laminates [25]. The efficiency of the CFRP strengthening method subjected to cyclic loading has been confirmed by enhanced moment capacity, stiffness, ductility, energy absorption and delayed local buckling of structural members [23,26]. The fatigue behaviour of the steel plates [28,29] and steel members [30] have been improved by strengthening with FRP. Moreover, the FRP strengthening technique also showed its effectiveness in enhancing the impact performance of steel members [31,32]. However, research into FRP retrofitting of welded beam-column connections subjected to monotonic loading and cyclic loading from earthquakes is a research area that has not been covered in the current literature.

Research in the area of CFRP strengthened steel I-section welded beam-column connection is relatively new and there is a shortage of investigation into their behaviour under monotonic and cyclic loading. Extensive research was conducted on FRP strengthened steel members subjected to cyclic loading [30,33–36], but relatively less done on FRP strengthened connections especially under large-displacement cyclic loading. In addition to the seismic deficiency of existing structures and their fatigue damage, failure of critical members in a steel building due to fracture are the major concern for designers. Moreover, structural members in a steel building might require strengthening due to deterioration of material properties under adverse environmental conditions, an increase in the service loads, or inadequate design of the steel members. The present paper addresses this research gap and evaluates the efficiency of CFRP strengthening on the performance of I-section connections subjected to monotonic and large-displacement cyclic loading. Towards this end, a series of experiments have been performed to investigate the performances of the full-scale bare and strengthened steel I-section welded beam-column connections under both monotonic and large-displacement cyclic loading. Carbon fibre reinforced polymer (CFRP) has been used in the present study as the strengthening material along with epoxy adhesive as the bonding material. The experimental

study conclusively showed the benefits of CFRP composites through enhanced performance of these welded connections under both monotonic and cyclic loading. Under monotonic loading, the ultimate moment capacity, stiffness, dissipation of energy and ductility of the welded connection has been enhanced due to CFRP strengthening. Additionally, under cyclic loading, the CFRP strengthened welded connections showed improved moment hysteresis behaviour, reduced degradation of the moment and higher stiffness and energy dissipation compared to their bare counterparts. The outcomes of this paper establish the benefits of CFRP composite and its application in retrofitting and strengthening steel beam-column connections and hence to provide enhanced performance under monotonic and cyclic loadings.

## **2. Experimental Program**

A series of full-scale experiments were carried out to investigate the behaviour of the bare and strengthened welded beam-column connections under monotonic and large-displacement cyclic loadings. Carbon fibre reinforced polymer (CFRP) is used as the strengthening material in the present study along with epoxy adhesive as the bonding material. The details of the experiment have been presented in this section.

### **2.1 Materials**

Four full-scale welded I-section connections were prepared to evaluate the performance of the bare and CFRP strengthened welded beam-column connections under monotonic and large-displacement cyclic loadings. Steel, epoxy adhesive and CFRP are the three different materials used in this research. The hot rolled universal beams and universal columns of Grade G300 were manufactured according to AS/NZS 3679.1 [37]. Steel coupons were prepared and tested by following AS1391 [38] to find out the steel mechanical properties. Average yield strength of 317 MPa, the elastic modulus of 203 GPa and tensile strength of 484.5 MPa were from the sample batch. Moreover, the average yield strain and ultimate strain of steel were 0.002 and

0.18 respectively. The MBrace Fib 300/50 CFS CFRP was used as the strengthening materials in the present study. Coupon testing of the epoxy cured CFRP laminates was conducted by one of the authors [39] following ASTM D3039-08 [40] to obtain the material properties of the CFRP composites. The measured tensile strength and elastic modulus of CFRP laminate were 987 MPa and 75 GPa respectively. The CFRP laminate thicknesses were measured from different locations with vernier callipers. The average of measured thicknesses of one-layer CFRP composites was 0.6 mm. Moreover, the manufacture has been provided the dry CFRP properties and taken from the available study [17]. The thickness, tensile strength and elastic modulus of dry CFRP were 0.176 mm, 3800 MPa and 240 GPa respectively [17]. To achieve the bonding between the CFRP layers and CFRP laminate to the steel surface, MBrace two-part saturant was used as an adhesive material. The mechanical properties of epoxy adhesive were measured by one of the authors [22] through coupon standard tensile tests according to ASTM: D638-10 [41]. The measured tensile strength and elastic modulus of epoxy adhesive were 46 MPa and 2.86 GPa respectively.

## **2.2 Experimental specimens and scheme of strengthening**

Welded I-section steel beam-column connection one of the most popular choices in rigid steel-framed structures especially in seismic risk regions. Those connections required higher strength and ductility capacity to withstand during earthquakes. The full-scale welded I-section steel beam-column connections used in the present investigation represented the standard beam-column assemblage occurring at various levels of the rigid steel-framed structures. Although considering heavy testing which nowadays is expensive and time-consuming, a full-scale experimental investigation is important to achieve more consistent and realistic outcomes with better precision. All four steel connections utilized identical 310 UB 32 as steel beams welded to identical 200 UC 46.2 steel columns. The lengths of the beam and column are 1000 mm and 1600 mm respectively. The strong column-weak beam concept was considered in choosing the

beam and column sections in which the nominal plastic moment capacity of the column is higher than that of the beam. The beam was welded to the flange of the column by following AS/NZS 1554.1 [42]. To connect the column ends to pinned supports, 25 mm thickness steel plates are welded to each end of the column. A total of four full-scale welded beam to column connections were prepared to test under monotonic and large-displacement cyclic loadings. Two connections remained bare to serve as control specimens while the other two connections were strengthened with CFRP.

Each specimen was labeled with an identifier containing two parts to identify types of beam-column connection and applied loading conditions. The first part is to identify the type of beam-column connection - BBCC means the bare connections whereas SBCC means CFRP strengthened connections. The second part is to identify applied loading condition - M means connections subjected to monotonic loading whereas C means connections subjected to cyclic loading. Table 1 represents the specimen details and the experimental matrix.

Table 1: Experimental connections matrix

Connection notation	Types of connection	Applied loading	Types of adhesive
BBCC-M	Bare connection	Monotonic	-
SBCC-M	Strengthened connection	Monotonic	Mbrace Saturant
BBCC-C	Bare connection	Cyclic	-
SBCC-C	Strengthened connection	Cyclic	Mbrace Saturant

All the connections were strengthened with three layers of FRP as results from previous studies showed that strengthening the CHS with three layers of CFRP is most effective under monotonic [9] and cyclic loadings [10]. Moreover, previous studies concluded that any further extension of the wrapping length after a certain bond length had little or no effect on the structural performance of steel members and suggested that adequate bond length can be



chosen between 200-300 mm [22]. Moreover, a previous study suggested strengthening the plastic hinge regions of the beams with CFRP [17] and the lengths of plastic hinge regions can be obtained as one-sixteenth of the span length of the steel frame [43]. Based on the above information and following available literature [44], the bond length of 300 mm along the beam extending from the column face was chosen to strengthen the beam and a bond length of 200 mm extending on each side of the column from the connection was chosen to strengthen the column. The CFRP fibres are applied with the first two layers running longitudinally with the beam to utilize the high tensile property of CFRP and the third layer wrapped in the lateral direction on the beam which will provide better confinement of the first two layers. This style of orientation has been chosen as it showed good performance in a previous study [22,45]. To obtain adequate confinement of the overlapped CFRP fibres coming from the beam, the first and third CFRP fibres on the column are applied horizontally along the column surfaces while the second layer is applied vertically along the column surface to best utilise the benefits of CFRP. Although CFRP's effective bond length, number of layers and layers orientation were already quantified for CFRP strengthened steel members [9,10,22], a detailed study can be conducted specifically on CFRP strengthened welded connection to quantify those parameters more precisely to strengthen the welded connections with CFRP as a future study. A schematic diagram of the test samples and the strengthening scheme are displayed in Figure 1.

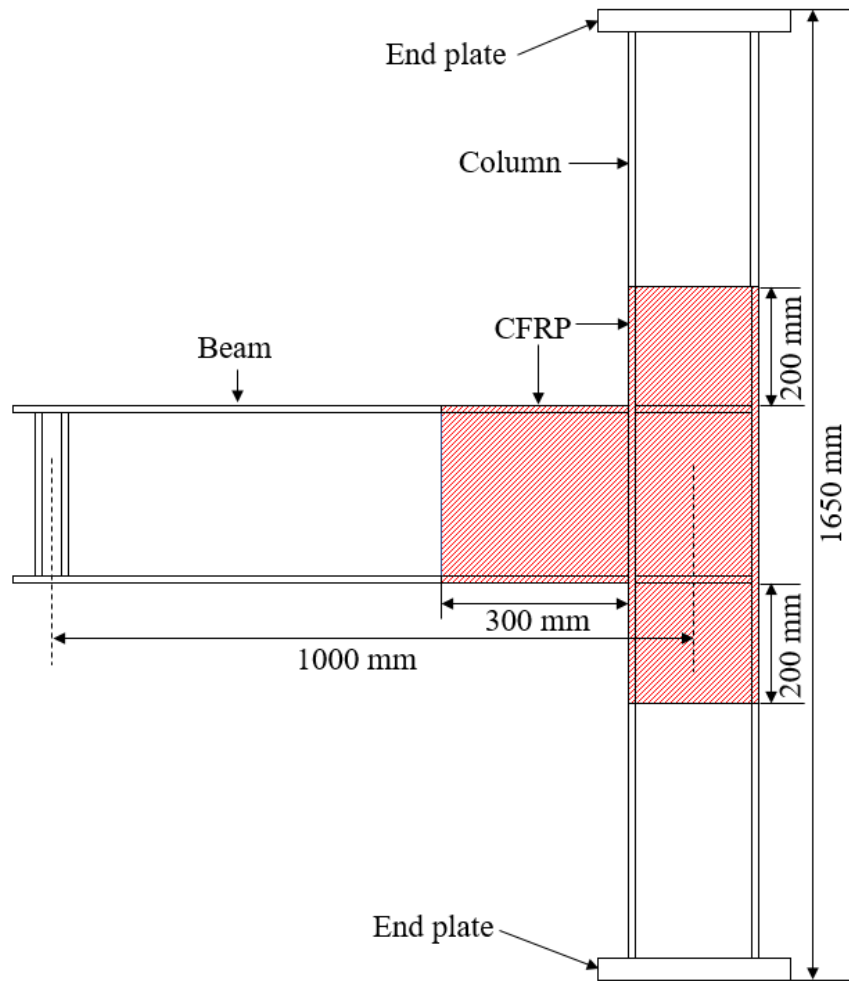


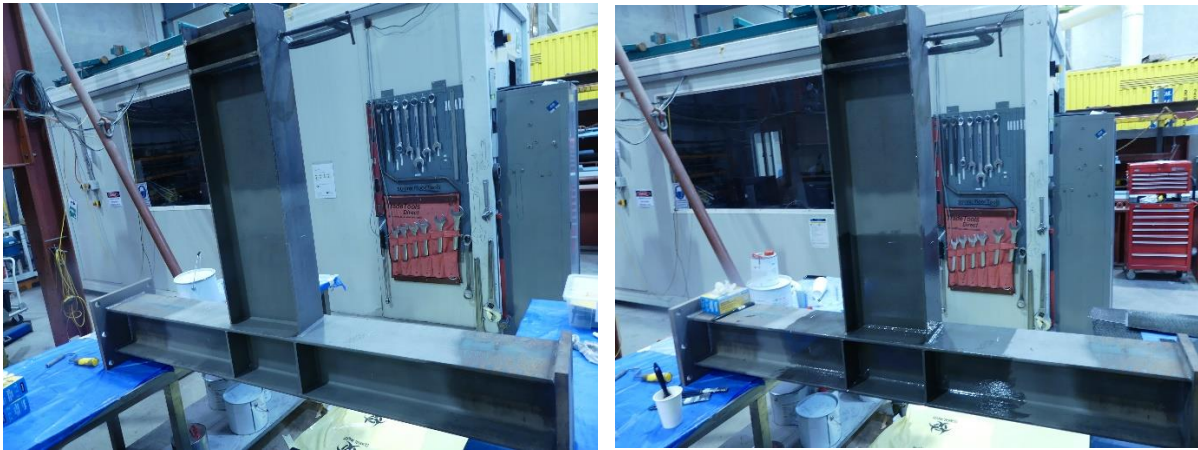
Figure 1: Schematic diagram of the FRP strengthened connection

### 2.3 Strengthening procedure

To ensure adequate bonding between the CFRP and steel, appropriate surface preparation of the steel connections was undertaken. Early studies reported sandblasting to be an effective method to remove the surface impurities from the steel [22,23,39]. The sandblasting method is very effective to obtain a uniform, high-energy finish to the steel surface which is very important for bonding between the steel and CFRP. This method is used in the current study for the welded connections surfaces. A local company was entrusted to sandblast the specimens as large surface areas required preparation. A granite abrasive was used for the sandblasting (grit no. 30/60) with an average grit size of 0.425 mm. Once the sandblasting was completed,

acetone was applied to the specimens to remove any dust particles or contaminants left on the surface. As in a previous study [22], good bonding between the CFRP and steel was achieved with this preparation. A sandblasted specimen can be seen in Figure 2(a), ready to be strengthened with CFRP. The prepared specimens were then treated with a two-part MBrace 3500 adhesion promoter primer followed by MBrace two-part 4500 epoxy adhesive. The two-part primer was mixed according to the guidelines of the manufacturer and after that applied to the steel surfaces of the connections using a brush. To develop a uniform and thin layer of primer, the specimens were brushed continuously every 5 to 10 minutes and then left to cure for 1 hour as shown in Figure 2(b) before the two-part epoxy adhesive was applied. Parts A and B of the epoxy adhesive were mixed for around 5 minutes to achieve a homogeneous mixture. The mixture was then applied on top of the primer layer which was already applied to the steel. The required sizes of CFRP sheets were prepared based on the wrapping scheme and applied on the adhesive wetted steel surfaces. Lengths of 50 mm overlap and 75 mm overlap were used on the members in the longitudinal and horizontal directions respectively. A rib roller, shown in Figure 2(c), was used while wrapping the CFRP and rolled in the direction of the fibre, removing entrapped air bubbles and impregnating the CFRP with the applied epoxy in the same process. Rib rolling was applied until the full saturation of the epoxy into the CFRP fabrics was achieved. A composite of the epoxy and CFRP plate was achieved once the curing of the specimen was complete. Managing the wrapping process time was important as the workability of this process is governed by the epoxy and its curing time. The specimens were strengthened with three layers of CFRP where the second and third layers were applied consecutively following the method used for the first layer. As this was a multilayer process, the wrapping was completed on the wet surface of the layer that preceded it. Thus, once cured, the multilayers of CFRP and epoxy acted as one single composite plate. Masking tape was applied as shown in Figure 2(d) immediately after finishing the strengthening work to prevent

premature debonding of the composite and ensure a uniform thickness between the epoxy resin and the CFRP laminate. Previous researchers [22,23,39] found the taping method to be extremely effective when applied to strengthened steel members. The masking tape was removed after 24 hours of curing and the specimens were left to further cure for 2 weeks prior to testing.



(a)

(b)



(c)

(d)

Figure 2: Specimen preparation: (a) connection after sandblasting; (b) Application of primer; (c) process of rib rolling; (d) application of masking tape

## **2.4 Experimental setup and loading protocol**

The experimental setup shown in Figure 4 was used to investigate the behaviour of both bare and CFRP strengthened welded connections under cyclic and monotonic loadings. In the test setup, the column member was mounted vertically and restrained by the supporting frame and the hydraulic actuator was positioned at the cantilevered end of the horizontal beam. The column was attached to the supporting frame through two hinged connections at either end of the column. Under these test conditions, it is possible to represent half the length of a column in a real structural frame, since it is possible to obtain approximately zero moments at the end of the column supports. To study the bending behaviour of the specimens without introducing an axial component to the loading, the displacement load input was applied through a two-pinned hinge connection clipped at the tip of the beam. The gusset plates were attached by welding between the flanges of the beam end at the displacement control loading point which helped to prevent deformation occurring locally during the application of the displacement control loading. An overall evaluation of the welded connections and their inelastic bending behaviour under monotonic and cyclic loading can be possible using the boundary conditions in the present experimental setup shown in Figure 4.

To apply the displacement control monotonic and large-displacement cyclic loading, a 1000kN hydraulic actuator was used in the experiments. Lasers displacement sensors (LDS) were used to measure the displacement of the beam tip and the flexibility of support connections. To study the moment rotation behaviour under cyclic loading of welded connections, an increasing large-displacement cyclic loading protocol ANSI/AISC 341-16 [5] was used as shown in Figure 5. This loading protocol simulated field-type earthquakes. This displacement-controlled loading protocol was applied at a quasi-static rate of 12.5 mm/min. The beam tip vertical displacement was divided by beam span length (1000 mm) to obtain the rotation of the connections. It was observed during the experiment that minor rigid rotations occurred at the

supports of the connection. The schematic diagram and the photograph in Figure 3 and Figure 4 respectively clearly show the details of the experimental setup used in the present study.

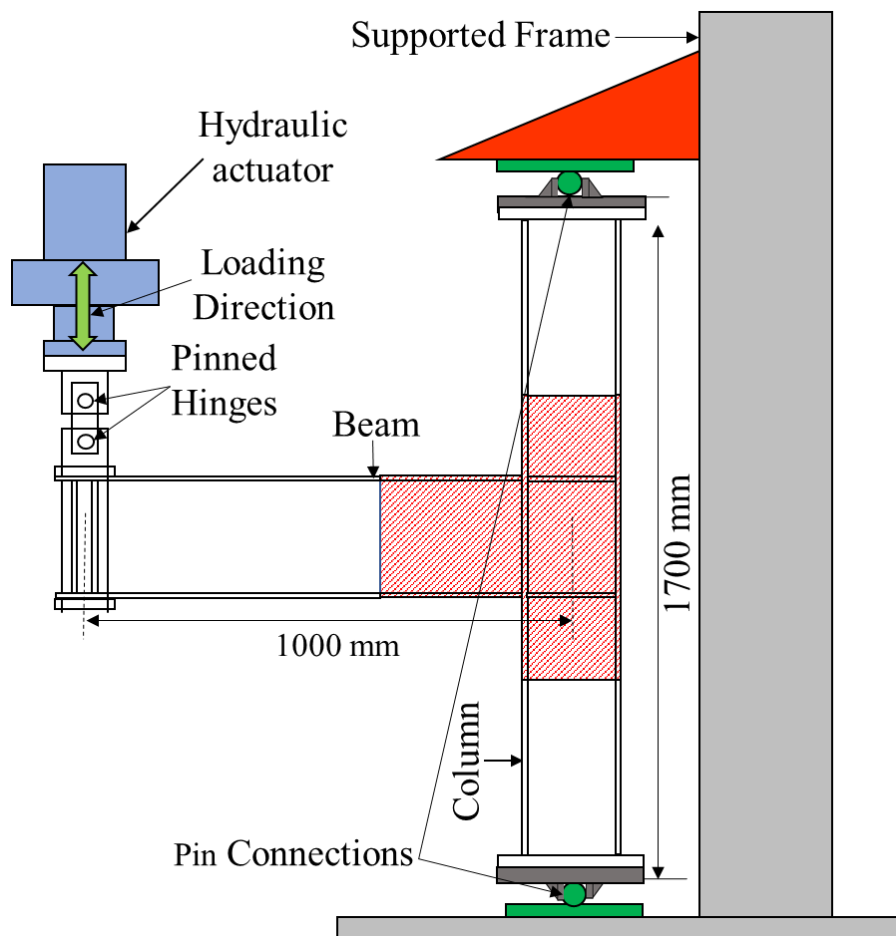


Figure 3: Schematic drawing of the experimental setup

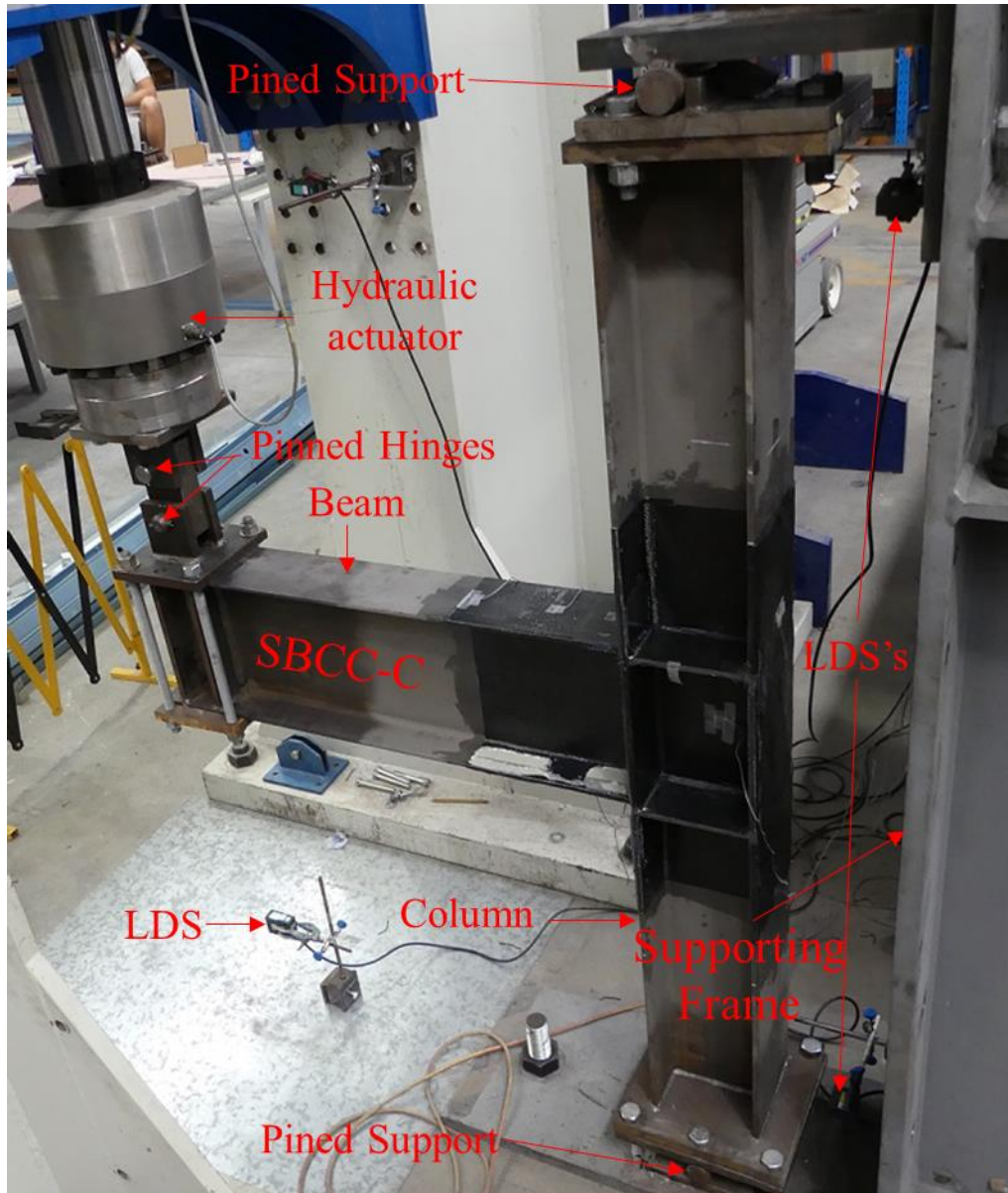


Figure 4: Photograph of the experimental setup

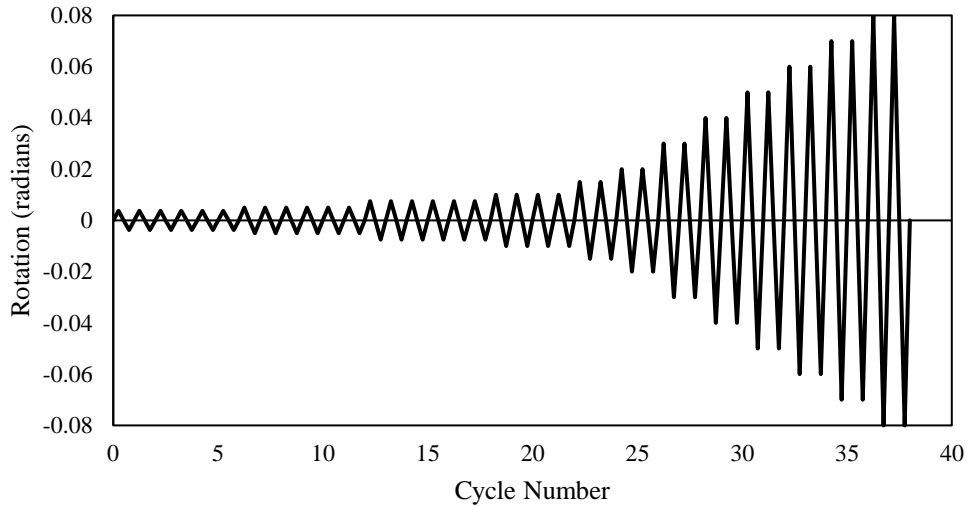


Figure 5: Cyclic loading protocol [5].

### 3. Experimental Results and Discussion

The experimental study conclusively showed the use of CFRP composites to enhance the performance of welded connections under both monotonic and cyclic loadings. Under monotonic loading, the ultimate moment capacity, stiffness, dissipation of energy and ductility of the welded connections were effectively improved by strengthening with CFRP. Additionally, under cyclic loading, the CFRP strengthened welded connections showed improvement in moment hysteresis behaviour, less degradation of the moment and higher stiffness and energy dissipation compared to their bare counterparts.

#### 3.1 Behaviour under monotonic loading

There is a clear benefit that can be seen noticed by strengthening the welded beam-column connection with CFRP under the monotonic loading test conditions. The CFRP strengthened welded connections exhibit improved structural behaviour compared to the bare welded connections. Moment-displacement graphs of the bare and CFRP strengthened connections are compared in Figure 6. The load applied to each specimen was multiplied by the lever arm (span length) of the beam (1000 mm) to calculate the moment in each specimen. CFRP strengthened



welded connection showed an improvement in moment capacity compared to the bare welded connection. The ultimate moment capacity of the CFRP strengthened welded connection is 212.1 kN.m which is an improvement of 21% compared to the ultimate moment capacity of 175.2 kN.m of the bare welded connection. This improvement is due to the composite action provided by the CFRP strengthening technique to the welded connection.

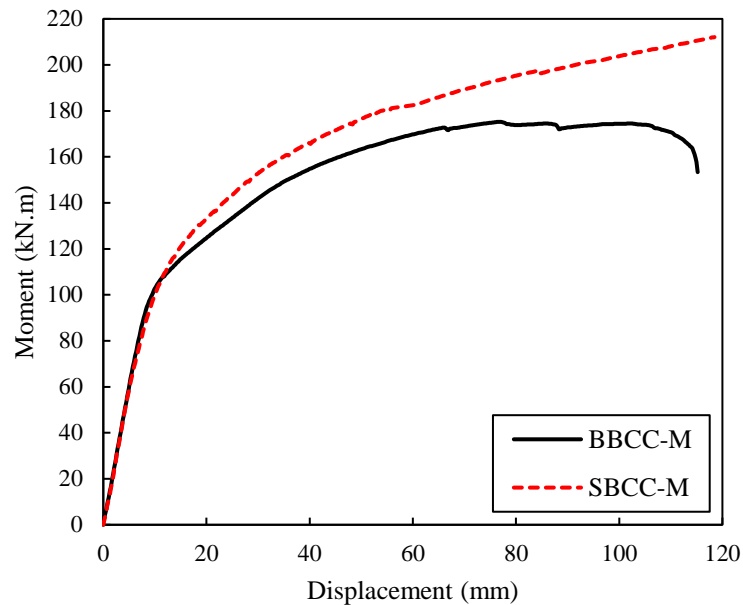
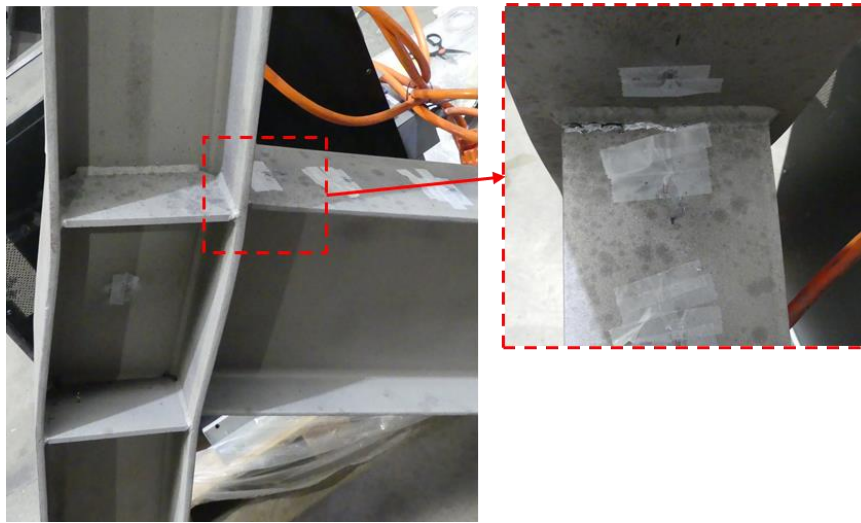


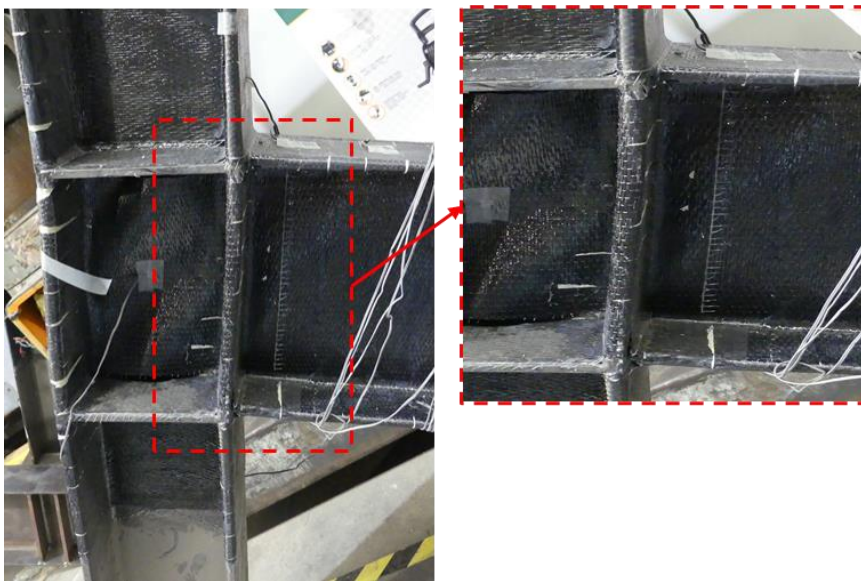
Figure 6: Moment-displacement curves of the bare and CFRP strengthened welded connections under monotonic loading

The failure modes of the bare and CFRP strengthened connections under monotonic loading are shown in Figure 7. In the bare connection, fracture initiated near the corner of the flange at the toe of the CJP weld after reaching the ultimate moment capacity at a displacement of 76.7 mm. The fracture propagated away from the corner towards the centre of the flange with increasing displacement and can be seen in Figure 7(a). The composite action and stiffness provided by the CFRP strengthening technique prolonged the fracture initiation and reached the ultimate moment capacity at a displacement of 118.5 mm. Significant distortion can be seen in the panel zones of both bare and CFRP strengthened connections. Mele et al. [46] and Fadden

et al. [7] also observed similar modes of failure for welded connection under cyclic loading. Moreover, debonding of CFRP has been observed in the panel zone area.



(a)



(b)

Figure 7: Failure modes of (a) bare connection and (b) CFRP strengthened connection under monotonic loading

The secant stiffness is the ratio of the load capacity and the corresponding displacement and calculated for both bare and CFRP strengthened welded connections. Figure 8 provides a comparison of the secant stiffness between the bare and CFRP strengthened welded

connections. The secant stiffness of the bare welded connection dropped by 88.9% from its maximum stiffness of 12027.6 kN/m to 1331.6 kN/m. On the other hand, the CFRP strengthened the welded connection dropped by 84.6% from its maximum stiffness of 11884.5 kN/m to 1827.5 kN/m. At the maximum displacement (in the present tests), the CFRP strengthened connection showed 37.24% higher secant stiffness compared to the bare connection by maintaining a smaller degradation of the secant stiffness.

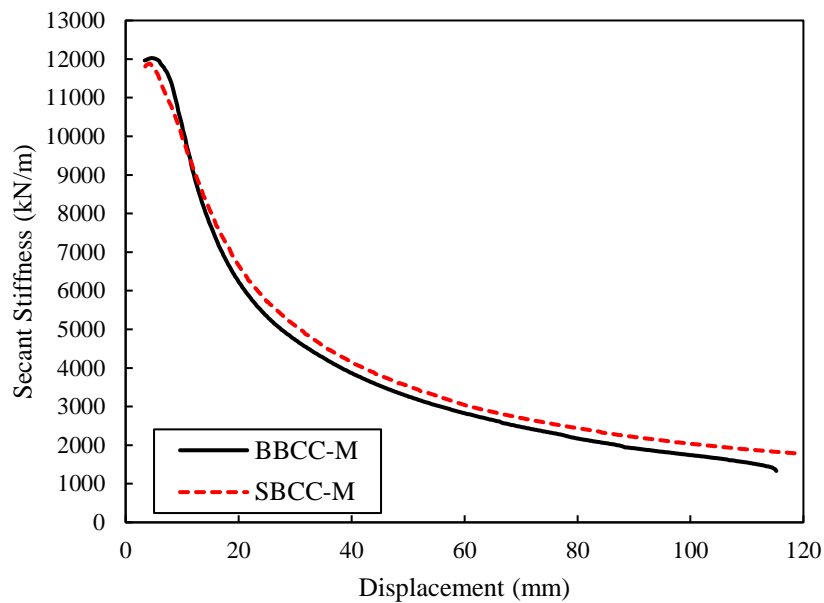


Figure 8: Secant stiffness-displacement curves of the bare and CFRP strengthened welded connections under monotonic loading

Energy dissipation by structural members during seismic events is mainly through inelastic deformation. Frame structures dissipate energy through the deformation of beams, columns, braces and panel zones. It is important to investigate the capacity of bare and CFRP strengthened connections to dissipate energy during a seismic event. The capacity to dissipate energy for each specimen was calculated at each stage by dividing the load capacity by the corresponding displacement at the particular displacement level. Figure 9 plots the comparison of energy dissipation capacity of the bare and CFRP strengthened connection with respect to

the displacement steps. Both the bare and CFRP strengthened connections indicated increasing energy dissipation across the full range of displacements which indicated that they both have the capacity for energy dissipation up to the final recorded displacement. The dissipated energy is small for both connections up to about the 5 mm displacement due to their high initial stiffness. At displacement level up to about 25 mm, the both bare and CFRP strengthened connections dissipated almost the same energy, probably because both beam-column connections behaved elastically during this phase. Before reaching the ultimate moment capacity of the bare connection, the energy dissipated by the CFRP strengthened connection is slightly higher than that of the bare connection. This shows that although the CFRP strengthened connection is initially stiff, it still influences the energy dissipation capacity. It becomes clear after reaching the ultimate moment capacity point of the bare connection that the CFRP strengthened connection has a much higher energy capacity than the bare connection. At the maximum displacement of bare connection, the energy dissipation of the CFRP strengthened connection is 19.9 kN.m, while the bare connection achieved a maximum of 17.5 kN.m which indicated that an overall improvement of 13.7% in energy dissipation capacity occurred due to CFRP strengthening. This shows that the earthquake performance of the CFRP strengthened connection to be superior compared to the bare connection although a parametric study is required to utilise the CFRP strengthening with maximum benefit. Moreover, at the ultimate moment point, the energy dissipation for bare connection is 10.7 kN.m and at the CFRP connection's ultimate moment point the energy dissipation is recorded as 19.9 kN.m, which shows an increase of 86.8% through CFRP strengthening.

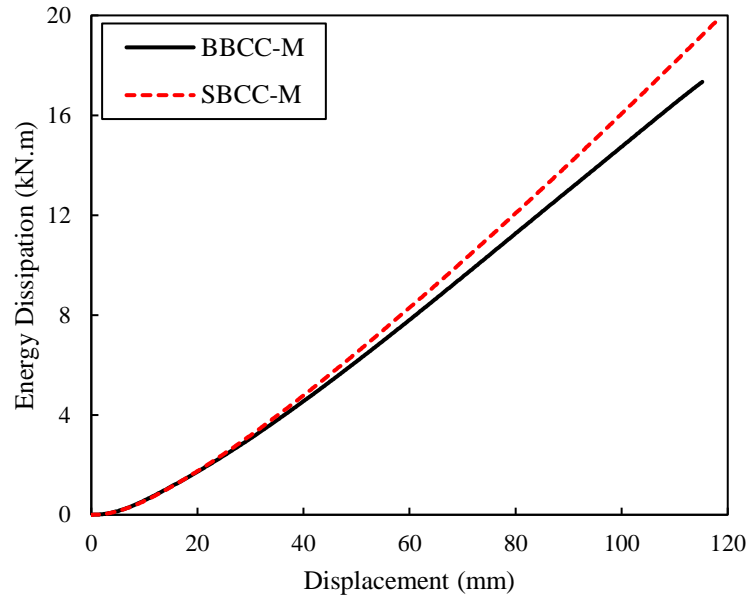


Figure 9: Energy dissipation-displacement curves of the bare and CFRP strengthened welded connections under monotonic loading

For earthquake-resisting members, ductility is an important parameter to be considered. The welded connections must exhibit adequate ductility and moment capacity during seismic activity. The ductility factor is the ratio between the dissipated energy determined at maximum load and the energy at the yield point. A larger ductility factor means that a member is more ductile. The method available in [47] was used to locate the yield point and Figure 10 provides a comparison of the ductility factor between the bare and CFRP strengthened connections. The CFRP strengthened connection is seen to have a significantly increased ductility factor compared to the bare connection. The ductility factor of the bare connection is 5.13, whereas the CFRP strengthened connection achieved a ductility factor of 6.83. The CFRP strengthening technique increased the ductility of the connection by 33.7%. This means a strengthened connection will absorb more energy compared to the bare connection and perform better under

seismic conditions. Moreover, it is important to conduct a parametric study to get more benefits from CFRP strengthening technique.

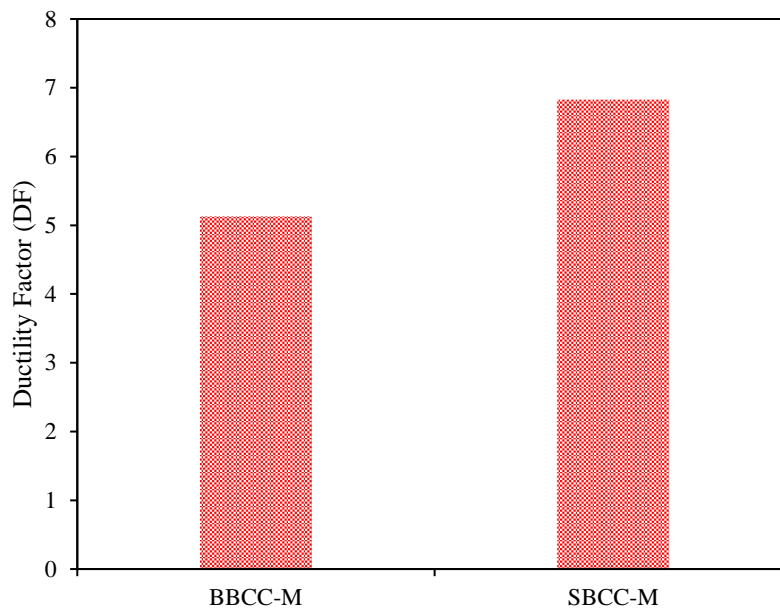


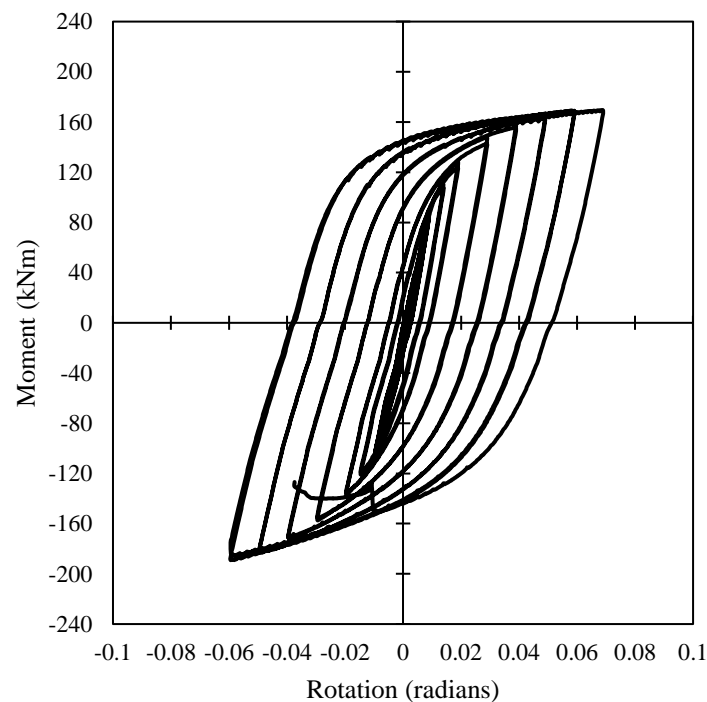
Figure 10: Ductility factors of the bare and CFRP strengthened welded connections under monotonic loading

### 3.2 Behaviour under cyclic loading

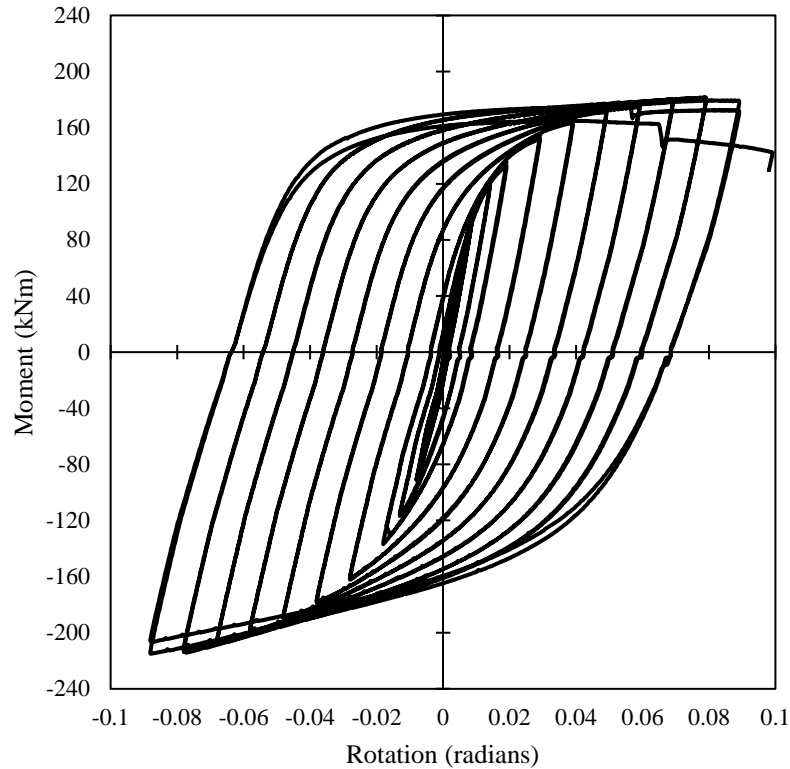
There is clear evidence that CFRP strengthened connection provide better performance under monotonic loading condition compared to their bare counterpart. To simulate seismic events more realistically, further investigation on the behaviour of the bare and CFRP strengthened connections under cyclic loading was undertaken. Cyclic hysteretic behaviours of the bare and strengthened connections are investigated in terms of moment capacities and their degradation, secant stiffness and energy dissipation to evaluate the efficiency of the CFRP strengthening method.

### 3.2.1 Experimental hysteretic behaviour

The hysteretic moment-rotational analysis of the bare and CFRP strengthened connections was conducted to evaluate the cyclic bending behaviour of the connections. The moment capacity was determined as the product of the applied load and the 1000 mm lever arm of the beam. Moment-rotation hysteresis curves of the bare and CFRP strengthened connections are plotted in Figure 11(a) and Figure 11(b) respectively. The maximum moment capacity is increased in the CFRP connection compared to the bare steel connection. In the positive rotational direction, the bare connection reached the maximum capacity of 169.6 kN.m, while the CFRP has a 7% higher moment capacity of 181.3 kN.m. In the negative direction, the bare and CFRP strengthened connections reached maximum moment capacities of 189.1 kN.m and 214.2 kN.m respectively, with the CFRP strengthened connection exhibiting a 13.2% greater moment capacity. Hence, the CFRP strengthening technique exhibited better performance under monotonic loading compared to the cyclic loading as the moment capacity of the connection improved by 21% under monotonic loading compared to 13.3% under cyclic loading.



(a)



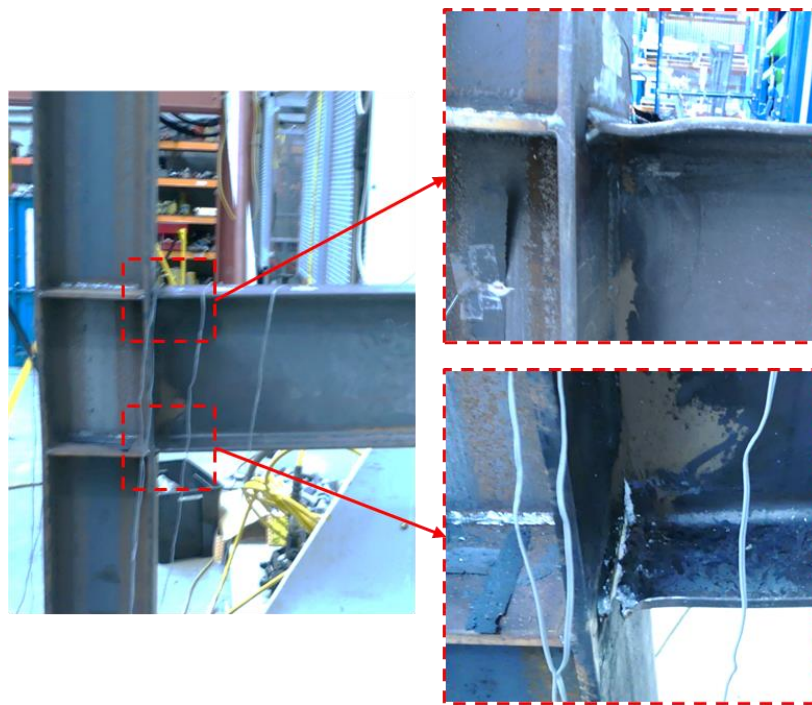
(b)

Figure 11: Moment capacity-rotation hysteresis curves of the (a) bare (b) CFRP strengthened connections

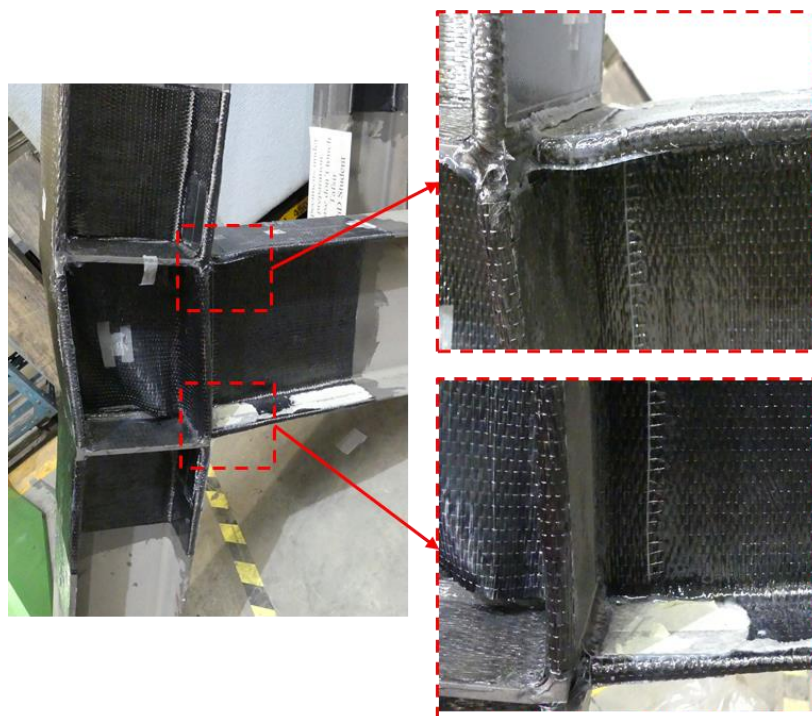
Figure 12 shows the failure modes of the bare and CFRP strengthened connections under cyclic loading. Both bare and CFRP strengthened connections did not show the degradation of strength and stiffness properties with the increasing number of cycles up to failure. The brittle failure mode, due to fracture close to the weld, with a sudden and sharp decrease of moment capacity at the very last cycle was noticed in both connections. The fracture has initiated in the beam flange and propagated in the web. Moreover, local buckling in the flange and a considerable distortion of the panel zone were also observed in the connections. Similar failure modes of welded connections under cyclic loading were observed in a previous study [7,46]. Moreover, debonding of CFRP has been observed in the panel zone area. Before the failure, the rotational capacities of the bare and CFRP strengthened connection were 0.07 and 0.09 radians respectively. Hence, the CFRP strengthened connection achieved higher rotational



capacity compared to the bare connection before failure due to the stiffness provided by the CFRP.



(a)



(b)

Figure 12: Failure modes of (a) bare connection and (b) CFRP strengthened connection under cyclic loading

The above responses are captured and compared through backbone plots shown in Figure 13 which emphasizes the hysteretic behaviour outcomes of Figure 11. Moment vs rotation curves for both the CFRP strengthened and bare connections are displayed as backbone curves in Figure 13 in which the moment at the maximum rotation of the first cycle of each rotational level is plotted against the corresponding rotation. These curves show a small asymmetry between the positive and negative regions due to some flexibility at the column end supports and the loading point. For the positive rotational direction, the increment of moment capacity of the bare connection starts to be stable after the rotation of 0.03 radians and reaches its maximum moment capacity of 168.5 kN.m at 0.06 radians. For the CFRP strengthened connection the increment of moment capacity starts to become stable after the rotation of 0.03 radians and reaches its maximum moment capacity of 181.3 kN.m at 0.08 radians. In contrast, for the negative rotational direction, the increment of moment capacity of the bare connection starting to be stable after the rotation of 0.04 radians and reached its maximum moment capacity of 189.0 kN.m at 0.06 radians. For the CFRP strengthened connection the increment of moment capacity starting to be stable after the rotation of 0.04 radians and reached its maximum moment capacity of 214.1 kN.m at 0.09 radians.

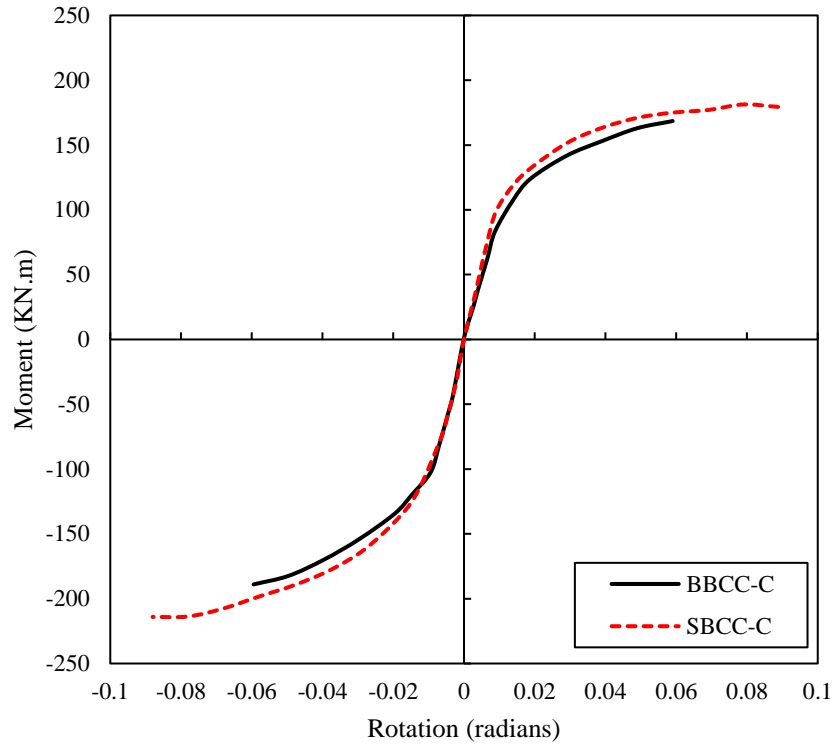


Figure 13: Moment capacity-rotational hysteresis backbone curves of the bare and CFRP strengthened connections

### 3.2.2 Secant Stiffness

The CFRP strengthening method also showed its ability to enhance the secant stiffness of the bare connection. The secant stiffness at a particular rotational level is calculated as the ratio of the load at maximum displacement to that maximum displacement. Figure 14 showed a comparison of the secant stiffness between the bare and CFRP strengthened connections. The CFRP strengthened method influenced the secant stiffness by increasing the welded connections stiffness. The maximum stiffness of the CFRP strengthened connection is 10873 kN/m at 0.01 radians which is 14.1% higher compared to the maximum stiffness 9526.1 kN/m of the bare connection at the same 0.01 radians. At the ultimate moment of the bare connection (0.06 radian), the stiffness of the bare and CFRP strengthened connections are 2856.4 kN/m and 2972.5 kN/m respectively, with the CFRP strengthening showing 4.1% higher stiffness. Consequently, in the negative rotational direction, the maximum stiffness of the bare and CFRP

strengthened connections are obtained as 10891.6 kN/m and 11345.9 kN/m respectively at the same rotational level of 0.01 radians, and hence a 4.2% improvement in the stiffness is indicated due to CFRP strengthening. At the ultimate moment of the bare connection (0.06 radians) in the negative rotational direction, the stiffness of the CFRP strengthened connection is 3420.1 kN/m which is 7.7% higher than the stiffness of 3176.4 kN/m of the bare connection, indicating an enhanced stiffness of the CFRP strengthened connection under cyclic loading.

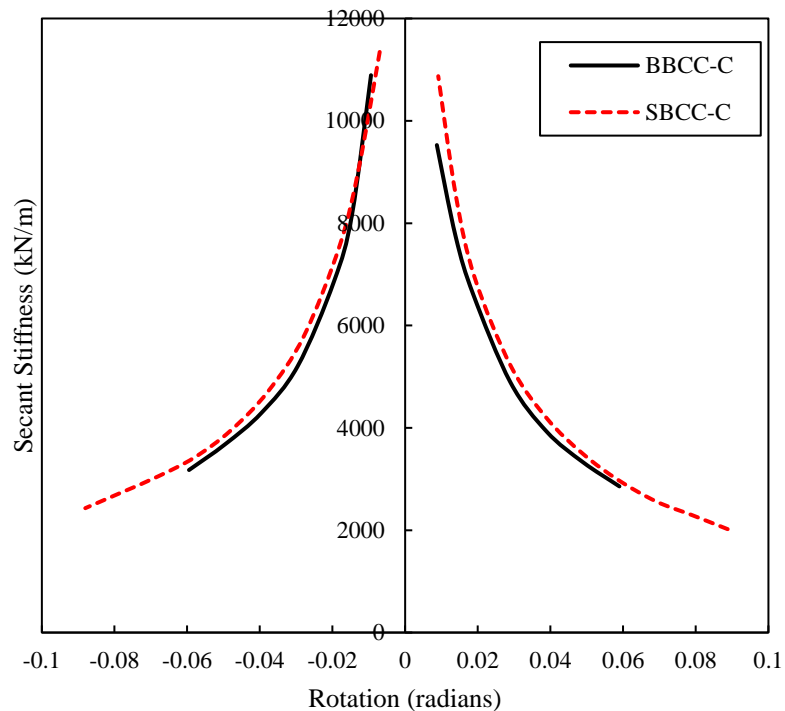


Figure 14: Secant stiffness-rotation curves of the bare and CFRP strengthened connections

### 3.2.3 Energy Dissipation Capacity

In a steel structure, seismic energy typically gets dissipated via inelastic deformation of the structural elements. Consideration of the energy dissipation capacity during the evaluation of the member capacity is, therefore, an important parameter for both bare and strengthened members. For a particular rotational level, the energy dissipation capacity is calculated by measuring the total enclosed area of all hysteresis loops in that particular rotational level and then plotting it against the rotational level. Figure 15 provides a comparison of the energy

dissipation capacity between the bare and CFRP strengthened connections. Both connections are able to generate hysteretic curves to the end of the cycle, which indicates that they both have the capacity for energy dissipation. The energy dissipation remained insignificant for both bare and CFRP strengthened connections up to 0.01 radians. This is due to both connections behave elastically until that rotational level. Clearly, the CFRP strengthened connection dissipated more energy compared to the bare connection at the ultimate moment loading. At the end of the experiment or the max rotational level of both connections, the bare and CFRP strengthened connections achieved energy dissipations of 47.9 kN.m and 87.3 kN.m respectively. Hence, the energy dissipation capacity increased by 82.2% due to the CFRP strengthening and confirmed that the CFRP strengthened connection is more stable and superior under seismic loading compared to the unreinforced bare connection.

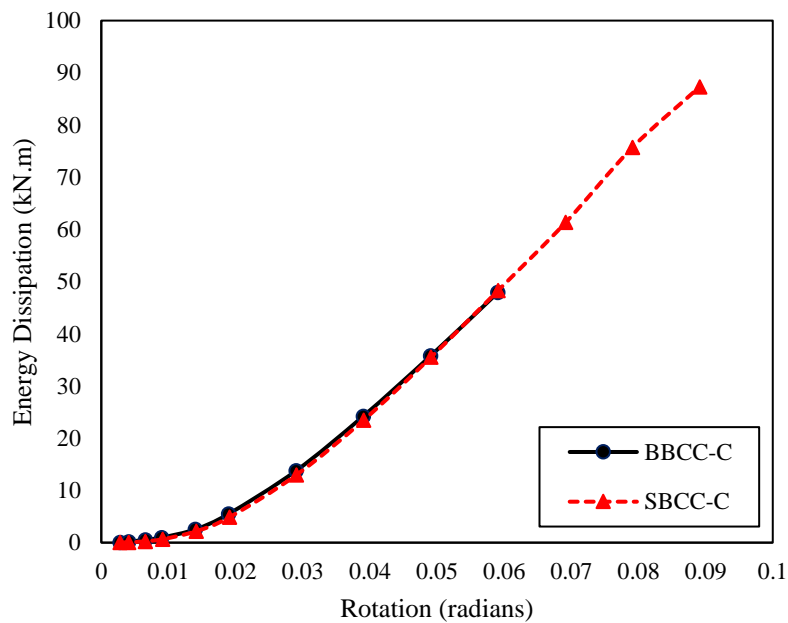


Figure 15: Energy dissipation-rotational curves of the bare and CFRP strengthened connections

#### 4. Comparison of experimental moment capacity with theoretically predicted moment capacity

The moment capacity of the beam members of the connections is calculated by following the AS4100 [48]. The thickness of the supplemented area of CFRP to steel ( $t_{es}^{(cs)}$ ) has been calculated according to Haedir et al. [21] and the transformed section of the CFRP strengthened I section is shown in Figure 16.

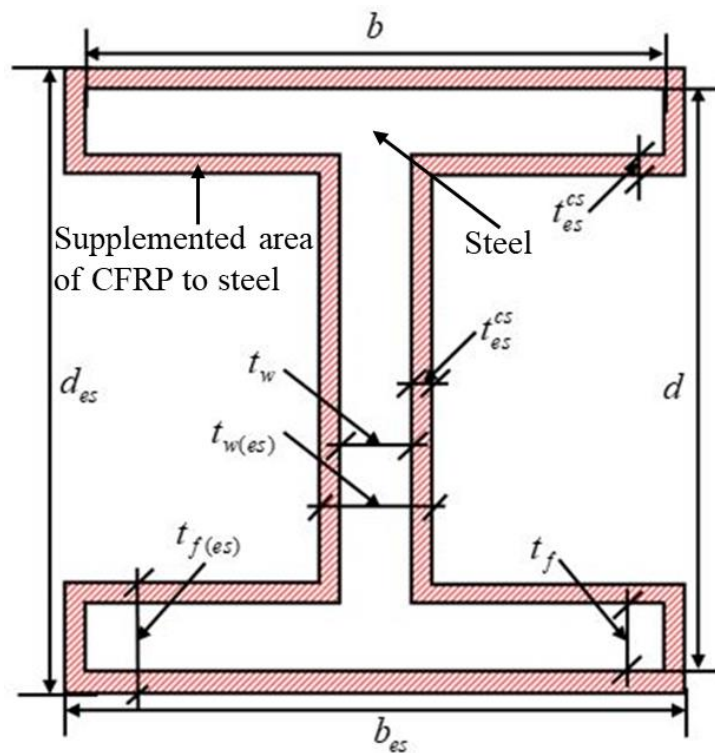


Figure 16: Transformed I section of CFRP strengthened I section

According to AS4100 [48], the elastic section modulus ( $Z$ ) and plastic section modulus ( $S$ ) of the compact steel I section can be expressed by equation (1) and (2) respectively and given below:

$$Z = \frac{bd^3}{6} + \frac{(b-t_w)(d-2t_f)^3}{6} \quad (1)$$

$$S = bt_f(d-t_f) + 0.25t_w(d-2t_f)^2 \quad (2)$$

Now, the elastic section modulus ( $Z_{es}$ ) and plastic section modulus ( $S_{es}$ ) of the equivalent section of CFRP strengthened section can be expressed by equation (3) and (4) respectively and given below:

$$Z_{es} = \frac{b_{es} d_{es}^3}{6} + \frac{(b_{es} - t_{w(es)}) (d_{es} - 2t_{f(es)})^3}{6} \quad (3)$$

$$S_{es} = b_{es} t_{f(es)} (d_{es} - t_{f(es)}) + 0.25 t_{w(es)} (d_{es} - 2t_{f(es)})^2 \quad (4)$$

where the dimensions of the equivalent section are  $b_{es} = b + 2t_{es}^{(cs)}$ ,  $d_{es} = d + 2t_{es}^{(cs)}$ ,

$$t_{f(es)} = t_f + 2t_{es}^{(cs)}, \quad t_{w(es)} = t_w + 2t_{es}^{(cs)}.$$

Then according to the AS4100 [48], the effective section modulus for the bare I section is the lesser of  $S$  or  $1.5 Z$  and the effective section modulus for CFRP strengthened I section is the lesser of  $S_{es}$  or  $1.5 Z_{es}$ . Then the moment capacity of the beam section of the connections has been calculated by multiplying the effective section modulus with the steel yield strength when the CFRP composite properties have been considered and shown a reasonable matching with the experimental moment capacity. On the other hand, when the dry CFRP properties have been considered, the moment capacity of the beam section of the connections has been calculated by multiplying the effective section modulus with the average of steel yield strength and ultimate strength by assuming some kind of strain hardening and shown a reasonable matching with the experimental moment capacity. The comparisons between theoretically predicted and experimental moment capacity based on both CFRP composite and dry properties are shown in Table 2. The experimentally obtained moment capacities match reasonably well with the theoretical predictions but are somewhat on the conservative side as the CFRP and weld around the joint are contributed to resistance.

Table 2: Comparison of experimental moment capacity with theoretically predicted moment capacity

Connections identification	Ultimate Moment capacity (kN.m)				$\frac{M_{Theo}}{M_{EXP}}$	
	Experimental ( $M_{EXP}$ )	Theoretical ( $M_{Theo}$ )		Based on CFRP composite properties		
		Based on CFRP composite properties	Based on CFRP dry properties			
BBCC-M	175.20	150.58	150.58	0.86	0.86	
SBCC-M	212.10	196.89	204.58	0.93	0.96	
BBCC-C	189.10	150.58	150.58	0.80	0.80	
SBCC-C	214.20	196.89	204.58	0.92	0.96	
				Mean Ratio	0.88	0.89
				COV	0.06	0.08

## 5. Conclusions

Strengthening steel structures with CFRP is a relatively new solution and offers extensive benefits over traditional strengthening methods. This area however lacks extensive research on the effects of CFRP strengthened welded steel beam-column connection subjected to monotonic loading and large-displacement cyclic loading. The behaviour of bare and CFRP strengthened welded connections have been experimentally investigated under monotonic and cyclic loading in the present study. From the results of the experimental study, it can be concluded that the CFRP strengthening technique is very effective in improving the behaviour of welded steel connections under both monotonic and cyclic loadings. The outcomes and major observations of the study have been summarised in the following:



- The moment capacity of the CFRP strengthened connection increased significantly over that of its bare counterpart under monotonic loading, resulting in a 21% increase in the ultimate moment capacity.
- CFRP strengthening improved the secant stiffness of the connection under monotonic loading. At the end displacement of the bare connection, the CFRP strengthened welded connection showed 37.24% higher secant stiffness compared to the bare connection by maintaining a smaller degradation compared to the bare connection.
- The earthquake performance of CFRP strengthened connection to be superior compared to the unstrengthened bare connection as the energy dissipation capacity has enhanced by 13.7% due to CFRP strengthening.
- The CFRP strengthening technique increased the ductility of the steel connection by 33.7% under monotonic loading. This enhanced ductility of the CFRP strengthened connection indicates that it should perform better under earthquake and cyclic loading.
- The CFRP strengthened connection exhibited higher moment capacities of 7.2% and 13% respectively compared to its bare counterpart in the positive and negative rotational directions of cyclic loading.
- The CFRP strengthened welded connection exhibited better stiffness behaviour compared to the bare welded connection in both positive and negative rotational directions. It showed higher maximum stiffness and higher stiffness throughout all cycles as well compared to the bare connection.
- The energy dissipation capacity of steel connection increased by 82.2% under cyclic loading as a result of strengthening with CFRP and confirmed that the CFRP strengthened connection is more stable and superior under seismic loading compared to the unreinforced bare connection.

- The experimentally obtained moment capacities are reasonably close to the theoretical predictions but are slightly conservative as the CFRP composites and weld around the connection also contribute.

Moreover, the performance of CFRP strengthened full-scale steel beam-column connection under monotonic and large-displacement cyclic loading can be investigated numerically followed by a parametric study as a future study.

### **Acknowledgments**

The authors wish to thank the Queensland University of Technology (QUT), Australia for providing support to conduct currently reported experimental testing. The authors wish to thank the technical staff of the Banyo Pilot Plant Precinct of Queensland University of Technology (QUT), Mr. Frank De Bruyne, Mr. Barry Hume, Mr. Glenn Atlee, and Mr. Cameron Creevey, for their technical supports.

### **Data Availability Statement**

Shearing of the raw data of the present research is not possible at this stage as the outcomes of the present research are a part of an ongoing study.

### **Reference**

- [1] Parker M, Steenkamp D. The economic impact of the Canterbury earthquakes. *Reserv Bank New Zeal Bull* 2012;75:13–25.
- [2] Mahin S a. Lessons from damage to steel buildings during the Northridge earthquake. *Eng Struct* 1998;20:261–70. [https://doi.org/10.1016/S0141-0296\(97\)00032-1](https://doi.org/10.1016/S0141-0296(97)00032-1).
- [3] Youssef NFG, Bonowitz D, Gross JL. A survey of steel moment-resisting frame buildings affected by the 1994 Northridge earthquake. US National Institute of Standards and Technology; 1995.

- [4] Wang M, Shi Y, Wang Y, Shi G. Numerical study on seismic behaviors of steel frame end-plate connections. *J Constr Steel Res* 2013;90:140–52. <https://doi.org/10.1016/j.jcsr.2013.07.033>.
- [5] ANSI/AISC 341-16. *Seismic Provisions for Structural Steel Buildings*, 2016. <https://doi.org/111>.
- [6] Seica M V., Packer JA. FRP materials for the rehabilitation of tubular steel structures, for underwater applications. *Compos Struct* 2007;80:440–50. <https://doi.org/10.1016/j.compstruct.2006.05.029>.
- [7] Fadden M, Wei D, McCormick J. Cyclic Testing of Welded HSS-to-HSS Moment Connections for Seismic Applications. *J Struct Eng* 2014;141:04014109. [https://doi.org/10.1061/\(asce\)st.1943-541x.0001049](https://doi.org/10.1061/(asce)st.1943-541x.0001049).
- [8] Liu Y, Tafsirojjaman T, Dogar AUR, Hückler A. Shrinkage behavior enhancement of infra-lightweight concrete through FRP grid reinforcement and development of their shrinkage prediction models. *Constr Build Mater* 2020;258. <https://doi.org/10.1016/j.conbuildmat.2020.119649>.
- [9] Tafsirojjaman T, Fawzia S, Thambiratnam DP. Investigation on the behaviour of CFRP strengthened CHS members under Monotonic loading through finite element modelling. *Structures* 2020;28:297–308. <https://doi.org/10.1016/j.istruc.2020.08.059>.
- [10] Tafsirojjaman T, Fawzia S, Thambiratnam DP, Zhao XL. Study on the cyclic bending behaviour of CFRP strengthened full-scale CHS members. *Structures* 2020;28:741–56. <https://doi.org/10.1016/j.istruc.2020.09.015>.
- [11] Al-Fakih A, Hisbany Mohd Hashim M, Alyousef R, Mutafi A, Hussein Abo Sabah S, Tafsirojjaman T. Cracking behavior of sea sand RC beam bonded externally with CFRP

- plate. *Structures* 2021;33:1578–89. <https://doi.org/10.1016/j.istruc.2021.05.042>.
- [12] Elchalakani M, Karrech A, Basarir H, Hassanein MF, Fawzia S. CFRP strengthening and rehabilitation of corroded steel pipelines under direct indentation. *Thin Walled Struct* 2017;119:510–21. <https://doi.org/10.1016/j.tws.2017.06.013>.
- [13] Erdem I, Akyuz U, Ersoy U, Ozcebe G. An experimental study on two different strengthening techniques for RC frames. *Eng Struct* 2006;28:1843–51. <https://doi.org/10.1016/j.engstruct.2006.03.010>.
- [14] Corte G, Barecchia E, Mazzolani F. Seismic upgrading of RC buildings by FRP: full-scale tests of a real structure. *J Mater Civ Eng* 2006;18:659–69. [https://doi.org/10.1061/\(ASCE\)0899-1561\(2006\)18:5\(659\)](https://doi.org/10.1061/(ASCE)0899-1561(2006)18:5(659)).
- [15] Di Ludovico M, Prota A, Manfredi G, Cosenza E. Seismic strengthening of an under-designed RC structure with FRP. *Earthq Eng Struct Dyn* 2008;37:141–62.
- [16] Tafsirojjaman T, Fawzia S, Thambiratnam D. Enhancement Of Seismic Performance Of Steel Frame Through CFRP Strengthening. *Procedia Manuf* 2019;30:239–46. <https://doi.org/10.1016/j.promfg.2019.02.035>.
- [17] Tafsirojjaman T, Fawzia S, Thambiratnam D, Zhao XL. Seismic strengthening of rigid steel frame with CFRP. *Arch Civ Mech Eng* 2019;19:334–47. <https://doi.org/10.1016/j.acme.2018.08.007>.
- [18] Tafsirojjaman T, Fawzia S, Thambiratnam D. Numerical investigation on the cfrp strengthened steel frame under earthquake. *Mater Sci Forum* 2020;995:123–9. <https://doi.org/10.4028/www.scientific.net/MSF.995.123>.
- [19] Tafsirojjaman T, Fawzia S, Thambiratnam D. Numerical investigation on the seismic strengthening of steel frame by using normal and high modulus CFRP. *Proc. seventh*

Asia-Pacific Conf. FRP Struct., International Institute for FRP in Construction (IIFC); 2019.

- [20] Siddique MAA, El Damatty AA, El Ansary AM. A numerical investigation of overstrength and ductility factors of moment resisting steel frames retrofitted with GFRP plates. *Can J Civ Eng* 2014;41:17–31. <https://doi.org/10.1139/cjce-2012-0271>.
- [21] Haedir J, Bambach MR, Zhao XL, Grzebieta RH. Strength of circular hollow sections (CHS) tubular beams externally reinforced by carbon FRP sheets in pure bending. *Thin-Walled Struct* 2009;47:1136–47. <https://doi.org/10.1016/j.tws.2008.10.017>.
- [22] Kabir MH, Fawzia S, Chan THT, Gamage JCPH, Bai JB. Experimental and numerical investigation of the behaviour of CFRP strengthened CHS beams subjected to bending. *Eng Struct* 2016;113:160–73. <https://doi.org/10.1016/j.engstruct.2016.01.047>.
- [23] Tafsirojjaman T, Fawzia S, Thambiratnam D, Zhao XL. Behaviour of CFRP strengthened CHS members under monotonic and cyclic loading. *Compos Struct* 2019;220:592–601. <https://doi.org/10.1016/j.compstruct.2019.04.029>.
- [24] Kabir MH, Fawzia S, Chan THT. Durability of CFRP strengthened circular hollow steel members under cold weather: Experimental and numerical investigation. *Constr Build Mater* 2016;123:372–83. <https://doi.org/10.1016/j.conbuildmat.2016.06.116>.
- [25] Siddique MAA, El Damatty AA. Improvement of local buckling behaviour of steel beams through bonding GFRP plates. *Compos Struct* 2013;96:44–56. <https://doi.org/10.1016/j.compstruct.2012.08.042>.
- [26] Tafsirojjaman T, Fawzia S, Thambiratnam D, Zhao X. Numerical investigation of CFRP strengthened RHS members under cyclic loading. *Structures* 2020;24:610–26. <https://doi.org/10.1016/j.istruc.2020.01.041>.

- [27] Kabir MH, Fawzia S, Chan THT, Badawi M. Durability of CFRP strengthened steel circular hollow section member exposed to sea water. *Constr Build Mater* 2016;118:216–25. <https://doi.org/10.1016/j.conbuildmat.2016.04.087>.
- [28] Liu H, Xiao Z, Zhao XL, Al-Mahaidi R. Prediction of fatigue life for CFRP-strengthened steel plates. *Thin-Walled Struct* 2009;47:1069–77. <https://doi.org/10.1016/j.tws.2008.10.011>.
- [29] Feng P, Hu L, Zhao XL, Cheng L, Xu S. Study on thermal effects on fatigue behavior of cracked steel plates strengthened by CFRP sheets. *Thin-Walled Struct* 2014;82:311–20. <https://doi.org/10.1016/j.tws.2014.04.015>.
- [30] Hu L, Feng P, Zhao XL. Fatigue design of CFRP strengthened steel members. *Thin-Walled Struct* 2017;119:482–98. <https://doi.org/10.1016/j.tws.2017.06.029>.
- [31] Alam MI, Fawzia S, Tafsirojjaman T, Zhao XL. FE modeling of FRP strengthened CHS members subjected to lateral impact. *Tubul. Struct. XVI Proc. 16th Int. Symp. Tubul. Struct. (ISTS 2017, 4-6 December 2017, Melbourne, Aust., CRC Press; 2017, p. 409–14*.
- [32] Batuwitige C, Fawzia S, Thambiratnam DP, Tafsirojjaman T, Al-Mahaidi R, Elchalakani M. CFRP-wrapped hollow steel tubes under axial impact loading. *Tubul. Struct. XVI Proc. 16th Int. Symp. Tubul. Struct. (ISTS 2017, 4-6 December 2017, Melbourne, Aust., CRC Press; 2017, p. 401–8*.
- [33] Zhishen WGLHW, Haitao RYW. Experimental study of the fatigue performance of steel beams strengthened with different fiber reinforced polymers. *China Civ Eng J* 2012;4.
- [34] Wu G, Wang HT, Wu ZS, Liu HY, Ren Y. Experimental study on the fatigue behavior of steel beams strengthened with different fiber-reinforced composite plates. *J Compos*

- Constr 2012;16:127–37. [https://doi.org/10.1061/\(ASCE\)CC.1943-5614.0000243](https://doi.org/10.1061/(ASCE)CC.1943-5614.0000243).
- [35] Colombi P, Fava G. Fatigue crack growth in steel beams strengthened by CFRP strips. *Theor Appl Fract Mech* 2016;85:173–82. <https://doi.org/10.1016/j.tafmec.2016.01.007>.
- [36] Ghafoori E, Schumacher A, Motavalli M. Fatigue behavior of notched steel beams reinforced with bonded CFRP plates: Determination of prestressing level for crack arrest. *Eng Struct* 2012;45:270–83. <https://doi.org/10.1016/j.engstruct.2012.06.047>.
- [37] AS/NZS 3679.1. Structural steel – Part 1: Hot-rolled bars and sections, 2016.
- [38] AS 1391. Metallic materials-Tensile testing at ambient temperature, 2007.
- [39] Alam MI, Fawzia S, Zhao XL, Remennikov AM, Bambach MR, Elchalakani M. Performance and dynamic behaviour of FRP strengthened CFST members subjected to lateral impact. *Eng Struct* 2017;147:160–76. <https://doi.org/10.1016/j.engstruct.2017.05.052>.
- [40] ASTM D3039. Standard Test Method for Tensile Properties of Polymer Matrix Composite Materials, 2008.
- [41] ASTM D638. Standard Test Method for Tensile Properties of Plastics., 2010.
- [42] AS/NZS 1554.1. Structural steel welding Welding of steel structures, 2014.
- [43] Ribeiro FLA, Barbosa AR, Scott MH, Neves LC. Deterioration Modeling of Steel Moment Resisting Frames Using Finite-Length Plastic Hinge Force-Based Beam-Column Elements. *J Struct Eng* 2015;141:04014112. [https://doi.org/10.1061/\(ASCE\)ST.1943-541X.0001052](https://doi.org/10.1061/(ASCE)ST.1943-541X.0001052).
- [44] Tafsirojjaman T, Fawzia S, Thambiratnam DP, Zhao X-L. FRP strengthened SHS beam-column connection under monotonic and large-deformation cyclic loading. *Thin-Walled*

Struct 2021;161:107518. <https://doi.org/10.1016/j.tws.2021.107518>.

- [45] Tafsirojjaman T, Fawzia S, Thambiratnam DP, Wirth N. Performance of FRP strengthened full-scale simply-supported circular hollow steel members under monotonic and large-displacement cyclic loading. Eng Struct 2021;242:112522. <https://doi.org/10.1016/j.engstruct.2021.112522>.
- [46] Mele E, Calado L, De Luca A. Experimental Investigation on European Welded Connections. J Struct Eng 2003;129:1301–11. [https://doi.org/10.1061/\(ASCE\)0733-9445\(2003\)129:10\(1301\)](https://doi.org/10.1061/(ASCE)0733-9445(2003)129:10(1301)).
- [47] Li ZX. Theory and technique of engineering structure experiments. Tianjin Univ Press Tianjin 2004.
- [48] AS 4100. Steel structures, 2016.